arXiv:hep-ex/9907012v1 10 Jul 1999

The Structure of Quasi-Real and Virtual Photons *

Richard Nisius, *CERN, CH-1211 Genève 23, Switzerland, e-mail: Richard.Nisius@cern.ch*

This review covers the measurements of the QED and QCD structure of quasi-real and virtual photons from the reaction ee $\rightarrow$ ee$\gamma^{\star}\gamma^{(\star)} \rightarrow$ ee$X$, and is an update of the discussion presented in [1].

1. Introduction

One of the most powerful tools to investigate the structure of quasi-real photons, γ, is the measurement of photon structure functions in deep inelastic electron-photon scattering at electron-positron colliders, shown in Figure 1.
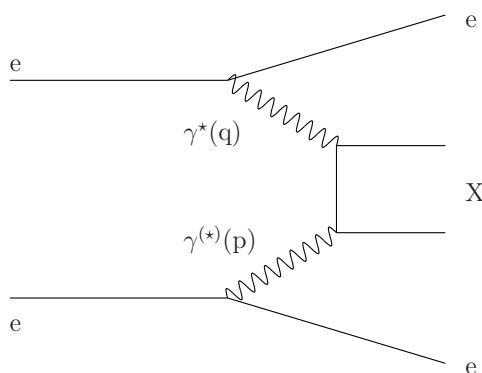

Figure 1.   A diagram of the reaction ee $\rightarrow$ ee$X$, proceeding via the exchange of two photons.

These measurements have by now a tradition of eighteen years since the first F_2^{γ} was obtained by PLUTO [2]. The LEP accelerator is a unique place for the measurements of photon structure functions until a high energy linear collider is realised. It is unique because of the large coverage in Q^2 owing to the various beam energies covered within the LEP programme, and due to the high luminosities delivered to the experiments. The main idea is that by measuring the differential cross-section

$$\frac{d^2\sigma_{e\gamma \rightarrow eX}}{dxdQ^2} = \frac{2\pi\alpha^2}{x\,Q^4}\left[\left(1+(1-y)^2\right)F_2^{\gamma}(x,Q^2) -y^2 F_{\rm L}^{\gamma}(x,Q^2)\right], \qquad (1)$$

one obtains the photon structure function F_2^{γ}. Here $Q^2 = -q^2$ is the absolute value of the four momentum squared of the virtual photon, $\gamma^{\star}$, x and y are the usual dimensionless variables of deep inelastic scattering and α is the fine structure constant. In the region of small y studied ($y \ll 1$) the contribution of the term proportional to $F_{\rm L}^{\gamma}$ is small and it is usually neglected. In leading order F_2^{γ} is proportional to the parton content, $f_{i,\gamma}$, of the photon, $F_2^{\gamma} = x\sum_{c,f} e_q^2 \left(f_{q,\gamma} + f_{\bar{q},\gamma}\right)$ for quarks, and therefore reveals the internal structure of the photon.

Because the energy of the quasi-real photon is not known, x has to be derived by measuring the invariant mass of the final state X, which consists of $\mu\mu$ pairs for the investigation of the QED structure of the photon, or of hadrons created by a quark pair in studies of F_2^{γ}. In the case of $\mu\mu$ final states the invariant mass can be determined accurately, and measurements of the QED structure are generally statistically limited. For hadronic final states the measurement of x is a source of significant uncertainties which makes measurements of F_2^{γ} mainly systematics limited.

If both photons are virtual an effective structure function $F_{\rm eff}^{\gamma}$ of virtual photons can be determined in the region $Q^2 \gg P^2 \gg \Lambda^2$ and, for $Q^2 \approx P^2 \gg \Lambda^2$ the differential cross-section for the exchange of two virtual photons is probed. Here Λ is the QCD scale. The different measurements performed to investigate the QED and QCD structure of the photon are discussed in the following.

---

2. The QED structure of the photon

Several measurements concerning the QED structure of the photon have been performed by various experiments. Prior to LEP, mainly $F_{2,\mathrm{QED}}^{\gamma}$ of quasi-real photons was measured. The LEP experiments refined the analysis of the $\mu\mu$ final state, and derived more information on the QED structure of the photon. The interest in the investigation of the QED structure of the photon is twofold. Firstly the investigations serve as tests of QED to order $\mathcal{O}(\alpha^4)$, but secondly, and also very important, the investigations are used to refine the experimentalists tools in a real but clean experimental situation to investigate the possibilities of extracting similar information from the much more complex hadronic final state.

2.1. The structure function $F_{2,\mathrm{QED}}^{\gamma}$

The structure function $F_{2,\mathrm{QED}}^{\gamma}$ has been measured using data in the approximate range of average virtualities $\langle Q^2 \rangle$ of $0.45 - 130$ GeV^2. Results were published by CELLO [3], DELPHI [4], L3 [5], OPAL [6], PLUTO [7] and TPC/2γ [8]. Additional preliminary results are available from ALEPH [9] and DELPHI [10]. The ALEPH results are preliminary since two years and therefore they are not considered here. The DELPHI result at $\langle Q^2 \rangle = 12.5$ GeV^2 is going to replace the published measurement, which will still be used here. Special care has to be taken when comparing the experimental results to the QED predictions, because slightly different quantities are derived by the experiments. Some of the experiments express their result as an average structure function, $\langle F_{2,\mathrm{QED}}^{\gamma}(x, Q^2) \rangle$, measured within their experimental acceptance in Q^2, whereas the other experiments unfold their result as a structure function for an average Q^2 value, $F_{2,\mathrm{QED}}^{\gamma}(x, \langle Q^2 \rangle)$. Figure 2 shows a summary of the $F_{2,\mathrm{QED}}^{\gamma}$ measurements compared either to $\langle F_{2,\mathrm{QED}}^{\gamma}(x, Q^2) \rangle$, assuming a flat acceptance in Q^2, or to $F_{2,\mathrm{QED}}^{\gamma}(x, \langle Q^2 \rangle)$, while using the appropriate values for Q^2 and $\langle Q^2 \rangle$ given by the experiments. For the measurements which quote an average virtuality $\langle P^2 \rangle$ of the quasi-real photon for their dataset, this value is chosen in the comparison, otherwise $P^2 = 0$ is used.
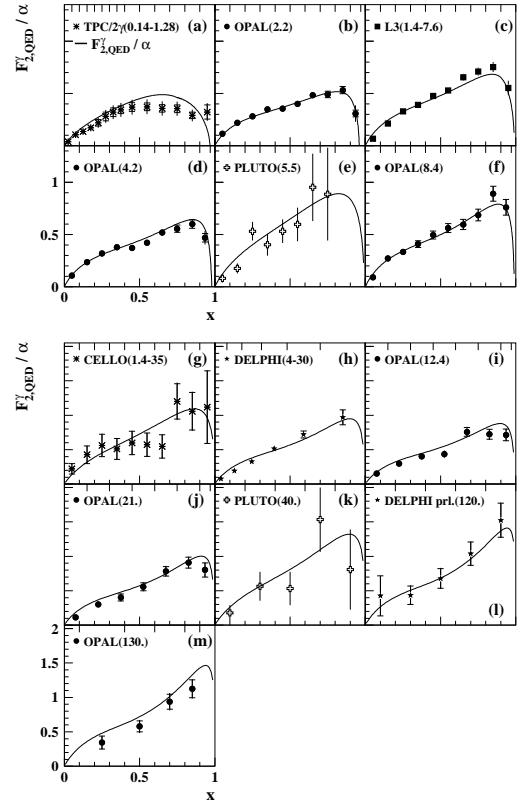

Figure 2. A summary of $F_{2,\mathrm{QED}}^{\gamma}$ measurements. The quoted errors for h) are statistical only.

There is agreement between the data and the QED expectations for about three orders of magnitude in Q^2. Some differences are seen for the TPC/2γ result, but at these low values of Q^2 this could also be due to the simple averaging procedure used for the theoretical prediction. The LEP data are so precise that the effect of the small virtuality of the quasi-real photon can clearly be established, as shown, for example, in Figure 3 for the most precise data from OPAL. The data are compared to the QED predictions of $F_{2,\mathrm{QED}}^{\gamma}(\mathrm{x}, \langle Q^2 \rangle, \langle P^2 \rangle, m_\mu)$, where either $\langle P^2 \rangle$ or m_μ is varied. The mass of the muon is found to be $m_\mu = 0.113\,^{+0.014}_{-0.017}$ GeV, assuming the $\langle P^2 \rangle$ value predicted by QED. Although this is not a precise measurement of the mass of the muon it can serve as an indication on the achievable precision for the determination of Λ, if it only were for the pointlike contribution to F_2^{γ}.
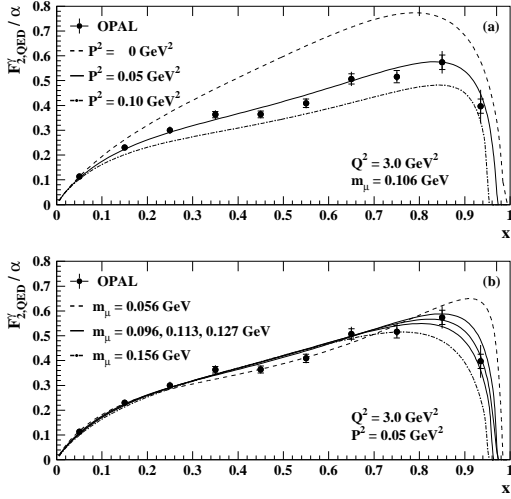
Figure 3. The dependence of $F_{2,\mathrm{QED}}^{\gamma}$ on P^2 and on the mass of the muon.

Figure 4. The measurements of $F_{A,\mathrm{QED}}^{\gamma}/F_{2,\mathrm{QED}}^{\gamma}$ and $1/2F_{B,\mathrm{QED}}^{\gamma}/F_{2,\mathrm{QED}}^{\gamma}$.

2.2. Azimuthal correlations

The structure functions $F_{A,\mathrm{QED}}^{\gamma}$ and $F_{B,\mathrm{QED}}^{\gamma}$ are obtained from the measured $F_{2,\mathrm{QED}}^{\gamma}$ and a fit to the shape of the distribution of the azimuthal angle χ, which is the angle between the plane defined by the momentum vectors of the muons and the plane defined by the momentum vectors of the incoming and the deeply inelastically scattered electron. For small values of y, the χ distribution can be written as:

$$\frac{\mathrm{d}N}{\mathrm{d}\chi} \sim 1 - A\cos\chi + B\cos 2\chi\,, \qquad (2)$$

with parameters $A = F_{A,\mathrm{QED}}^{\gamma}/F_{2,\mathrm{QED}}^{\gamma}$ and $B = 1/2F_{B,\mathrm{QED}}^{\gamma}/F_{2,\mathrm{QED}}^{\gamma}$. The recent theoretical predictions [11] which take into account the important mass corrections up to $\mathcal{O}(m_{\mu}^2/W^2)$ are consistent with the results from L3 [5] and OPAL [6] and with the preliminary results from DELPHI [10], as shown for the ratios in Figure 4. Both $F_{A,\mathrm{QED}}^{\gamma}$ and $F_{B,\mathrm{QED}}^{\gamma}$ are found to be significantly different from zero.

2.3. The cross-section for two exchanged virtual photons

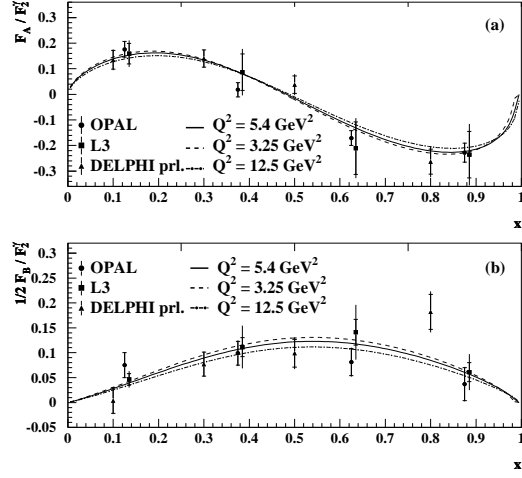The cross-section for the exchange of two highly virtual photons in the kinematical region under study can schematically be written as:

$$
\begin{aligned}
\sigma \quad \sim \quad & \sigma_{\mathrm{TT}} + \sigma_{\mathrm{TL}} + \sigma_{\mathrm{LT}} + \sigma_{\mathrm{LL}} + \\
& \frac{1}{2}\tau_{\mathrm{TT}}\cos 2\bar{\phi} - 4\tau_{\mathrm{TL}}\cos\bar{\phi}\,. \qquad (3)
\end{aligned}
$$

Here the total cross-sections σ_{TT}, σ_{TL}, σ_{LT} and σ_{LL} and the interference terms τ_{TT} and τ_{TL} correspond to specific helicity states of the photons (T=transverse and L=longitudinal), and $\bar{\phi}$ is the angle between the electron scattering planes. There is good agreement between the measured $\mathrm{d}\sigma/\mathrm{d}x$ from OPAL [6] and the QED predictions using the Vermaseren and the GALUGA Monte Carlo programs, provided all terms of the differential cross-section are taken into account. However, as apparent from Figure 5, if either τ_{TT} (dot-dash) or both τ_{TT} and τ_{TL} (dash) are neglected in the QED prediction as implemented in the GALUGA Monte Carlo, there is a clear disagreement between the data and the QED prediction. This measurement shows that both terms, τ_{TT} and especially τ_{TL}, are present in the data in the kinematical region of the analysis, mainly at $x > 0.1$, and that the corresponding contributions to the cross-section are negative.

As the kinematically accessible range in terms of Q^2 and P^2 for the measurement of the QED and the QCD structure of the photon is the same, and given the size of the interference terms in the
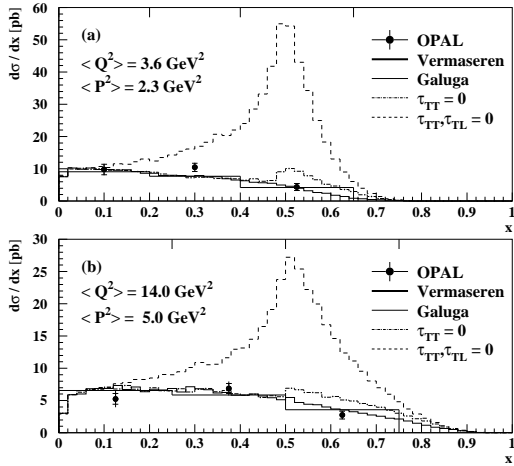
Figure 5. The measurement of the differential QED cross-section $d\sigma/dx$ for highly virtual photons.

Figure 6. The point-like (pl) and the hadron-like (had) contribution to F_2^γ as predicted by the GRV parametrisation.

leptonic case, special care has to be taken when the measurements on the QCD structure are interpreted in terms of hadronic structure functions of virtual photons.

3. The hadronic structure of the photon

The hadronic structure function F_2^γ contains two contributions from the different appearances of the resolved photon, namely the point-like component stemming from the point-like coupling of the photon to quarks, and the hadron-like component originating from the fluctuations of the photon into a hadronic state with the same quantum numbers as the photon. The hadron-like part can be modelled by Vector Meson Dominance and obeys the same evolution equations as the structure function of an ordinary hadron like the proton.

The composition of these two components predicted by the GRV parametrisation of F_2^γ is shown in Figure 6. With increasing Q^2 the hadron-like contribution dies out at large x and creates the steep rise at low x. In contrast, the point-like component increases with Q^2 at large x, the unique feature of F_2^γ compared to F_2^p. In the present investigations of F_2^γ both these features are investigated. The shape of F_2^γ as a function
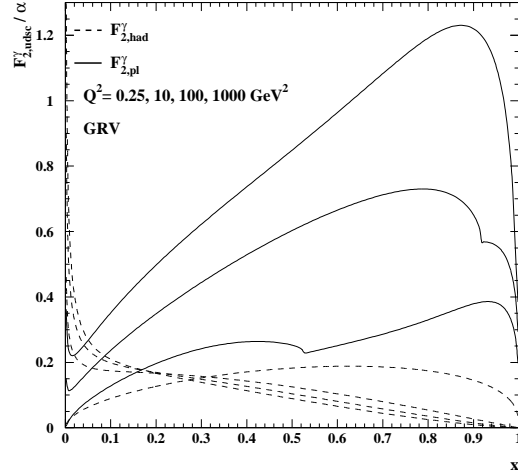
of x at fixed Q^2 is studied with emphasis on the low-x behaviour of F_2^γ in comparison to F_2^p, and the evolution of F_2^γ with Q^2 is measured mainly at medium x.

3.1. The description of the hadronic final state

The adequate description of the hadronic final state by the Monte Carlo models is very important for measurements of the photon structure. During the LEP2 workshop general purpose Monte Carlo programs became available for deep inelastic electron-photon scattering. The first serious attempt to confront these models with the experimental data has been performed by OPAL [12]. It was found, that none of the Monte Carlo programs available at that time was able to satisfactorily reproduce the data distributions. Therefore, the full spread of the predictions was included in the systematic error of the F_2^γ measurement, which consequently suffered from large systematic errors.

An important quantity is the flow of hadronic energy as a function of the pseudorapidity, $1/N \ dE/d\eta$. A significant fraction of the energy flow goes into the forward region of the detectors which are only equipped with electromag-

netic calorimeters. Given this, the detectors are precise enough to disentangle various predictions in the central part of the detector, however they are not able to distinguish very well between models which produce different energy flow distributions in the forward region.

The various Monte Carlo models produce significantly different hadronic energy flows, which leads to the fact that for a given value of W, the visible invariant mass W_{vis} is rather different when using different Monte Carlo models, with the largest differences occuring at low values of x.

In addition to the models discussed above the PHOJET and the TWOGAM Monte Carlo models were used in a structure function analysis from L3 [13], where the prediction of the hadronic energy flow for these two models was compared to the data for the Q^2 range $1.2 - 9$ GeV^2. Again, these two models, although closer to the data than the HERWIG5.8d and PYTHIA predictions in the case of the OPAL analysis, do not accurately account for the features observed in the data distributions.

Several methods were investigated to reduce the dependence on the Monte Carlo models:
• Motivated by the observation made in photoproduction studies at HERA [14], the HERWIG5.9 model was tuned [15] by changing the distribution of k_{t}, the intrinsic transverse momentum of the quarks inside the photon from a Gaussian to a power-law behaviour of the form $\mathrm{d}k_{\mathrm{t}}^2/(k_{\mathrm{t}}^2 + k_0{}^2)$. In the latest version the upper limit of k_{t} is dynamically adjusted on an event by event basis.
• The longitudinal momentum of the photon-photon system is unknown, but the transverse momentum is well constrained by measuring the transverse momentum of the scattered electron. This fact is used to replace a part of the measurement of the hadronic system by quantities obtained from the scattered electron, and thereby a part of the uncertainty of the measurement of the hadronic final state can be eliminated. The distribution of the invariant mass reconstructed in this scheme by L3 [13] is closer to the W distribution than the W_{vis} distribution, but still the agreement with W is not very good.

• Another way of reducing the model dependence is to perform the unfolding in two dimensions. Preliminary results from the ALEPH [16] and OPAL [17] experiments show that this indeed reduces the systematic uncertainty on the F_2^γ measurement.
• In order to establish a consistent picture a combined effort by the ALEPH, L3 and OPAL collaborations and the LEP Two-Photon Working Group has been undertaken [18]. The data of the experiments have been analysed in two regions of Q^2, $1.2 - 6.3$ GeV^2 and $6 - 30$ GeV^2, using identical cuts and also identical Monte Carlo events passed through the respective programs of the individual experiments to simulate the detector response. The data distributions are corrected to the hadron level, allowing for a direct comparison to the predictions of the Monte Carlo models. It was found, that for large regions in most of the distributions studied, the results of the different experiments are closer to each other than the sizable differences which are found between the data and the models.

From the discussion above it is clear, that the error on the measurement of F_2^γ will vary strongly with the Monte Carlo models chosen to obtain the systematic uncertainty. However, given the improved understanding of the shortcomings and the combined effort on improving on the Monte Carlo description of the data, it is likely that the error on F_2^γ will shrink considerably in future measurements.

3.2. The structure of quasi-real photons

Many measurements of the hadronic structure function F_2^γ have been performed at several electron-positron colliders. In this review the interpretation of the data will be based on the published results, and on those preliminary results from the LEP experiments, which are based on data which have not yet been published. For the preliminary results [17] which are meant to replace a published measurement in the near future the published result will be shown until the new result is finalised.

The range in $\langle Q^2 \rangle$ covered by the various experiments is $0.24 - 400$ GeV^2, which is impressive given the small cross-section of the process. In

Figure 7 the published results from ALEPH [19] AMY [20], DELPHI [4], JADE [21], L3 [13,22], OPAL [12,23,24], PLUTO [25], TASSO [26], TPC/2γ [27] and TOPAZ [28] are shown together with additional preliminary results from ALEPH [16], DELPHI [29] and L3 [30].

The precision of the measurements of F_2^γ which have been performed at e^+e^- centre-of-mass energies below the mass of the Z boson is mainly limited by the statistical error and, due to the simple assumptions made on the hadronic final state, the systematic errors are small, but in light of the discussion above, they maybe underestimated. Some of the data show quite unexpected features. For example, the F_2^γ as obtained from TPC/2γ shows an unexpected shape at low values of x, and also the results from TOPAZ rise very fast towards low values of x. In addition there is a clear disagreement between the TASSO and JADE data at $\langle Q^2 \rangle = 23 - 24$ GeV^2.
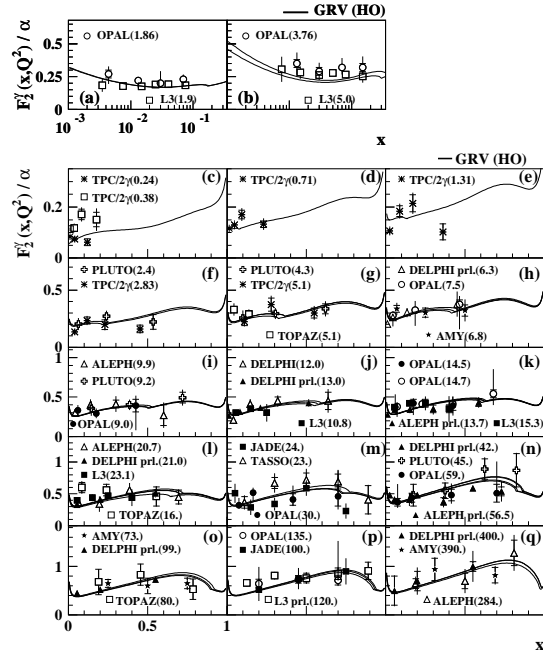

Figure 7. A summary of measurements of F_2^γ.

The measurement of F_2^γ has attracted a lot of interest at LEP over the last years. The LEP Collaborations have measured F_2^γ in the range $0.002 < x \lesssim 1$ and $1.86 < \langle Q^2 \rangle < 400$ GeV^2. As

seen from Figure 7 the measurements obtained at LEP1 energies (open symbols) are consistent with those obtained at LEP2 energies (closed symbols).

The comparison to the GRV higher order prediction of F_2^γ shows an overall agreement, but also some regions where the prediction does not so well coincide with the data. This large amount of data, which partly is rather precise, gives the possibility to study the consistency of the predictions with the data. The quality of the agreement is evaluated by a simple χ^2 method based on:

$$\chi^2 = \sum_i \left(\frac{F_{2,i}^\gamma - \langle F_2^\gamma(x, \langle Q^2 \rangle, 0) \rangle}{\sigma_i} \right)^2 , \qquad (4)$$

where the sum runs over all measurements in Figure 7 with $\langle Q^2 \rangle > Q_0^2$, where Q_0^2 is the starting scale of the evolution for the respective parametrisation of F_2^γ. The term $F_{2,i}^\gamma$ denotes the measured value of F_2^γ in the ith bin and σ_i is its total error. The theoretical expectation is approximated by the average F_2^γ in that bin in x for $Q^2 = \langle Q^2 \rangle$ and for $P^2 = 0$, abbreviated by $\langle F_2^\gamma(x, \langle Q^2 \rangle, 0) \rangle$. The procedure does not take into account the correlation of errors between the data points. A more accurate analysis would require to study in detail the correlation between the results within one experiment, but even more difficult, the correlation between the results from different experiments, a major task which is beyond the scope of the comparison presented here. The predictions used in the comparison are the WHIT parametrisations, which are the most recent parametrisations based on purely phenomenological fits to the data, and the GRV and SaS1D predictions which use some theoretical prejudice to construct the hadron-like part of F_2^γ at Q_0^2. The values of χ^2/dof found are: GRV LO (1.55), GRV HO (1.64), GRSchienbein LO (1.58), SaS1D (1.81), SaS1M (1.50), for $165/161$ data points with $\langle Q^2 \rangle > 0.38/0.71$ GeV^2, and SaS2D (0.97), SaS2M (1.01), WHIT1 (1.10), WHIT2 (3.27), WHIT3 (5.37), WHIT4 (5.78), WHIT5 (18.66), WHIT6 (28.29), for 132 data points with $\langle Q^2 \rangle > 4$ GeV^2. The parametrisations describe the AMY, JADE, PLUTO and TASSO data, and they all disfavour the TPC/2γ results. The WHIT parametrisations predict a

faster rise at low-x than the GRV, GRSc and the SaS parametrisations. Therefore, the agreement with the TOPAZ data is satisfactory for the WHIT parametrisations, whereas the GRV, GRSc and the SaS1 parametrisations yield values of χ^2/dof of around 2, and the SaS2 parametrisations lie somewhere between these extremes. For the same reason the WHIT parametrisations fail to describe the ALEPH and DELPHI data which tend to be low at low values of x, thereby leading to large χ^2/dof for the WHIT parametrisations, especially for the sets WHIT4-6 which use a larger gluon distribution functions. The only acceptable agreement is achieved by using the set WHIT1. The OPAL results tend to be high at low values of x and also they have larger errors, therefore only the extreme cases WHIT5-6 lead to unacceptable values of χ^2/dof. The quoted uncertainties by L3 are very small and the results tend to be high for low values of Q^2. Consequently, none of the parametrisations which are valid below $Q^2 = 4$ GeV^2 is able to describe the L3 data and all lead to large values of χ^2/dof. For $Q^2 > 4$ GeV^2 the agreement improves but the values of χ^2/dof are still too large, besides for GRSc. For the parametrisations valid for $Q^2 > 4$ GeV^2 the best agreement with the L3 data is obtained for WHIT1. This comparison shows that already at the present level of accuracy the measurements of F_2^γ are precise enough to constrain the parametrisations and to discard those which predict a fast rise at low x driven by large gluon distribution functions.

The second topic which is extensively studied using the large lever arm in Q^2, is the evolution of F_2^γ with Q^2. A collection of all available measurements of the evolution of F_2^γ at medium x for four active flavours is shown in Figure 8. For PLUTO the average $F_{2,\mathrm{c}}^\gamma$ in the range $0.2 < x < 0.8$ for the $\langle Q^2 \rangle$ values of the analyses has been added to the published three flavour result.

Unfortunately the different experiments quote their results for different ranges in x which makes the comparison more difficult because the predictions for the various ranges in x start to be significantly different for $Q^2 > 100$ GeV^2, as can be seen in Figure 8. The measurements are consis-

tent with each other and a clear rise of F_2^γ with Q^2 is observed. It is an interesting fact that this rise can be described reasonably well ($\mathcal{O}(15\%)$ accuracy) by the leading order augmented asymptotic prediction detailed in [23], which uses the asymptotic solution [31] for F_2^γ for the light flavour contribution as predicted by perturbative QCD for $\alpha_s(M_z^2) = 0.128$.
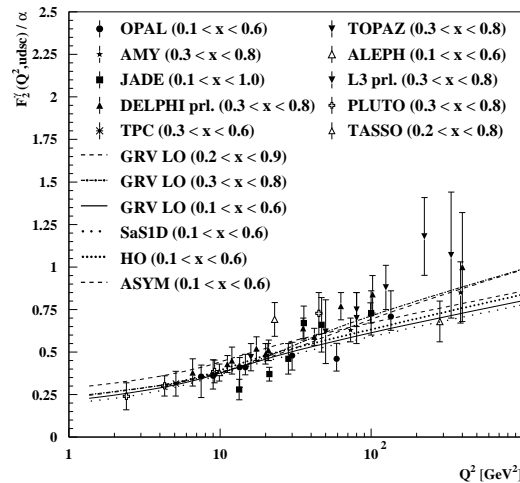

Figure 8. The Q^2 evolution of F_2^γ at medium x.

In order to look at the variation of the scaling violation as a function of x the data from Figure 7 are displayed differently in Figure 9. The data are shown as a function of Q^2, divided in bins of x, with average values as shown in the figure. Each individual measurement is attributed to the bin with the closest average value in x used. To separate the measurements from each other an integer value, N, counting the bin number is added to the measured F_2^γ. The theoretical prediction is the average F_2^γ in each bin. The Q^2 ranges used for the predictions are the maximum ranges possible for $1 < W < 250$ GeV and $Q_0^2 < Q^2 < 1000$ GeV^2. The general trend of the data is followed by the predictions of the augmented asymptotic solution, and the GRV and SaS1D leading order parametrisations of F_2^γ, however, differences are seen which were discussed above.
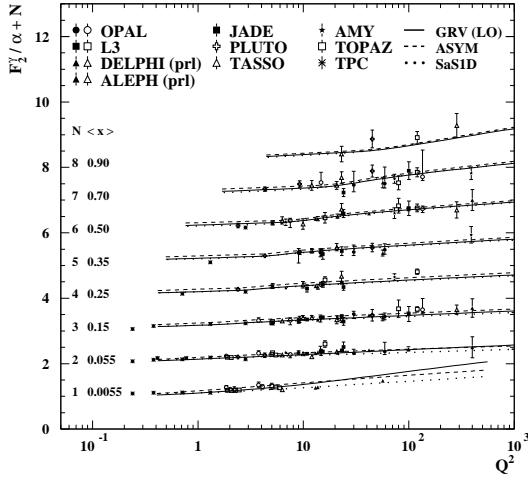
Figure 9. Summary of the measurements of the Q^2 evolution of F_2^γ.

3.3. The hadronic structure of virtual photons

The structure functions of virtual photons can be determined in the region $Q^2 \gg P^2$ by measuring the cross-sections for events where both electrons are observed. An effective structure function $F_{\text{eff}}^\gamma \propto \sigma_{\text{TT}} + \sigma_{\text{TL}} + \sigma_{\text{LT}} + \sigma_{\text{LL}} + 1/2\tau_{\text{TT}}\cos 2\bar\phi - 4\tau_{\text{TL}}\cos\bar\phi$ can be measured by experiments, however, to relate F_{eff}^γ to the structure functions F_2^γ and F_{L}^γ further assumptions are needed. By assuming that the interference terms do not contribute, that σ_{LL} is negligible and also using $\sigma_{\text{TL}} = \sigma_{\text{LT}}$, the relation $F_{\text{eff}}^\gamma = F_2^\gamma + 3/2F_{\text{L}}^\gamma$ is derived. Due to the P^2 suppression of the cross-section these measurements suffer from low statistics.

The first measurement of this type performed by PLUTO [32], for $\langle P^2 \rangle = 0.35$ GeV^2 and $\langle Q^2 \rangle = 5$ GeV^2, has been compared in [33] to the theoretical predictions from the GRS parametrisations. The best description of the data is obtained using the next-to-leading order result including a non-perturbative input at the starting scale of the evolution. If the hadron-like input is neglected, the prediction is consistently lower than the data, but still consistent with it, within the experimental errors. Also the prediction obtained by calculating F_{eff}^γ solely from the box diagram is still consistent with the data although it

is the lowest at high values of x. The evolution of F_{eff}^γ with P^2 has been studied as well, including the result of F_2^γ for the quasi-real photon. The data suggest a slow decrease with increasing P^2, but they are also consistent with a constant behaviour. Also for the P^2 evolution of F_{eff}^γ the full next-to-leading order prediction gives the best description of the data and the purely perturbative prediction is at the low end.

A similar measurement has been presented by L3 [30]. The average virtualities for the L3 result are $\langle Q^2 \rangle = 120$ GeV^2 and $\langle P^2 \rangle = 3.7$ GeV^2, thereby ensuring $Q^2 \gg P^2 \gg \Lambda^2$. As in the case of PLUTO the QPM result is too low compared to the data. Taking only F_2^γ as calculated from the GRS parametrisation of the parton distribution functions of the photon gets closer to the data, and the best description is found if the contribution of F_{L}^γ is added to this, based on the prediction of the QPM. The data show a faster rise with x than any of the predictions, however with large errors for increasing x, which are mainly due to the low statistics available.

The QPM prediction of the P^2 evolution of F_{eff}^γ is consistent in shape with the data, but the predicted F_{eff}^γ is too low. However, the main difference comes from F_2^γ at $P^2 = 0$, which is not described by the quark parton model for $x < 0.4$, where the hadron-like component is expected to be largest. But in this region the data are even higher than the predictions of all parametrisations of F_2^γ which contain a hadron-like contribution. The measurement at $P^2 > 0$ cannot rule out the quark parton model prediction, although the data are consistently higher. The ratio of $\langle Q^2 \rangle / \langle P^2 \rangle$ is similar for the PLUTO and L3 measurements, leading to values for $\ln(\langle Q^2 \rangle / \langle P^2 \rangle)$ of 2.6 and 3.5 respectively. This enables to compare the Q^2 evolution of the two measurements. The evolution is consistent with the expectation of the quark parton model for $\ln(\langle Q^2 \rangle / \langle P^2 \rangle) = 3$, and using the range $0.05 < x < 0.98$.

In summary a consistent picture is found for the effective structure function of the virtual photon between the PLUTO and L3 data and the general features of both measurements are described by the next-to-leading order predictions. However, the data do not constrain the predictions very

strongly and for more detailed comparisons to be made the full statistics of the LEP2 programme has to be explored.

If both photons have similar virtualities the application of the photon structure function picture is no longer applicable and the data are interpreted in terms of the differential cross-section. Due to the large virtualities the cross-section is small and large integrated luminosities are needed to precisely measure it. The main interest is the investigation of the hadronic structure of the interaction of two virtual photons. However, the interest in performing these measurements increased considerably in the last years, because calculations in the framework of the leading order BFKL evolution equation, which sums $\ln(1/x)$ contributions, predicted a large cross-section [34]. The predicted cross-section is so large that already measurements with low statistics are able to decide whether the BFKL picture is in agreement with the measurements. Recently theoretical progress has been made [35] to also include next-to-leading order pieces in the BFKL calculations [36]. Large negative corrections to the leading order results were found, e.g. [37], consequently, there is some doubt about the perturbative stability of the calculation. The theoretical development is underway and this should be kept in mind in comparisons to the BFKL predictions. The most suitable region for the comparison is $W^2 \gg Q^2 \approx P^2 \gg \Lambda^2$, which ensures similar photon virtualities and large values of $1/x$. These requirements strongly reduce the available statistics, therefore compromises have to be made in this comparisons.

The first measurement of this type was performed by L3 [38] using data at $\sqrt{s_{\rm ee}} = 91$ and 183 GeV, and additional preliminary results were reported [39] for data taken at $\sqrt{s_{\rm ee}} = 189$ GeV. The average photon virtualities $\langle Q^2 \rangle, \langle P^2 \rangle$ are 3.5, 14 and 14.5 GeV^2 respectively. The W ranges used are $2 - 30/5 - 70/5 - 75$ GeV for the three centre-of-mass energies, which means the lowest values of x probed are about $2 - 3 \cdot 10^{-3}$. The differential cross-section as a function of $Y = \ln(W^2/\sqrt{Q^2 P^2})$ is described by the TWOGAM Monte Carlo at $\sqrt{s_{\rm ee}} = 91$ and 183 GeV. The PHOJET model gives an adequate description at

$\sqrt{s_{\rm ee}} = 183$ and 189 GeV, whereas it fails to describe the data at $\sqrt{s_{\rm ee}} = 91$ GeV, probably due to the low cut in W applied. The prediction of the QPM is found to be too low at all energies. The cross-sections predicted by the BFKL calculation are much higher than what is observed and are strongly disfavoured by the data.

A similar analysis was presented by OPAL [40], based on data at $\sqrt{s_{\rm ee}} = 189$ GeV, with average photon virtualities of about 10 GeV^2, and for $W > 5$ GeV. The differential cross-section is obtained as functions of W, x and Q^2, for $W > 5$ GeV and for energies of the scattered electrons larger than 65 GeV, and polar angles in the range $34 - 55$ mrad. The measured cross-section in this region is $0.32 \pm 0.05(stat)^{+0.04}_{-0.05}(sys)$ pb, compared to the predicted cross-sections of 0.17 pb for PHOJET and 2.2/0.26 pb based on the BFKL calculation in leading/'higher order'. Also for OPAL the data are described by the PHOJET model and there is no room for large additional contributions. The precision of the results is limited by statistics and they can be improved by using the full statistics of the LEP2 programme.

4. Conclusions

Many new results on the QED and QCD structure of the photon have been obtained in the last years.

The QED predictions of the structure of the photon are found to be in good agreement with all experimental results.

For the measurement of the hadronic structure function F_2^γ considerable progress has been made concerning the problem of the inaccurate modelling of the hadronic final state by the Monte Carlo models. New results on the low-x behaviour of F_2^γ have been presented and by now the evolution of F_2^γ with Q^2 is probed up to $Q^2 = 400$ GeV^2.

Interesting studies on the hadronic structure of the exchange of two virtual photons have been performed. The effective structure function has been measured at LEP and its behaviour can be described by the next-to-leading order prediction. The cross-section for the exchange of two highly virtual photons can be described with conven-

tional models, whereas the present BFKL predictions are strongly disfavoured by the data.

Acknowledgement:

I wish to thank the organisers of this interesting conference for the fruitful atmosphere they created throughout the meeting.

REFERENCES

1. R. Nisius, in *DIS99 Conf., Zeuthen*, World Scientific, 1999, hep-ex/9905059; *DIS98 Conf., Brussels*, eds. G. Coremans and R. Roosen, pages 194–198, World Scientific, 1998; and *ICHEP97 Conf., Jerusalem*, 1997, hep-ex/9712012.
2. PLUTO Collab., C. Berger et al., Phys. Lett. **107B**, 168–172 (1981).
3. CELLO Collab., H.J. Behrend et al., Phys. Lett. **126B**, 384–390 (1983).
4. DELPHI Collab., P. Abreu et al., Z. Phys. **C69**, 223–234 (1996).
5. L3 Collab., M. Acciarri et al., Phys. Lett. **B438**, 363–378 (1998).
6. OPAL Collab., G. Abbiendi et al., CERN-EP/99-010.
7. PLUTO Collab., C. Berger et al., Z. Phys. **C27**, 249–256 (1985).
8. TPC/2γ Collab., M.P. Cain et al., Phys. Lett. **147B**, 232–236 (1984).
9. ALEPH Collab., C. Brew, in *Photon '97, Egmond aan Zee*, eds. A. Buijs and F.C. Erné, pages 21–26, World Scientific, 1998.
10. DELPHI Collab., A. Zintchenko, these proceedings.
11. R. Nisius and M.H. Seymour, Phys. Lett. **B452**, 409–413 (1999).
12. OPAL Collab., K. Ackerstaff et al., Z. Phys. **C74**, 33–48 (1997).
13. L3 Collab., M. Acciarri et al., Phys. Lett. **B436**, 403–416 (1998).
14. ZEUS Collab., M. Derrick et al., Phys. Lett. **B354**, 163–177 (1995).
15. J.A. Lauber, L. Lönnblad, and M.H. Seymour, in *Photon '97, Egmond aan Zee*, eds. A. Buijs and F.C. Erné, pages 52–56, World Scientific, 1998; S. Cartwright, M.H. Seymour, et al., J. Phys. G **24**, 457–481 (1998).
16. ALEPH Collab., A. Böhrer, these proceedings.
17. OPAL Collab., E. Clay, these proceedings.
18. ALEPH, L3 and OPAL Collabs., A. Finch, these proceedings.
19. ALEPH Collab., D. Buskulic et al., CERN-EP/99-063.
20. AMY Collab., S.K. Sahu et al., Phys. Lett. **B346**, 208–216 (1995); T. Kojima et al., Phys. Lett. **B400**, 395–400 (1997).
21. JADE Collab., W. Bartel et al., Z. Phys. **C24**, 231–245 (1984).
22. L3 Collab., M. Acciarri et al., Phys. Lett. **B447**, 147–156 (1999).
23. OPAL Collab., K. Ackerstaff et al., Phys. Lett. **B411**, 387–401 (1997).
24. OPAL Collab., K. Ackerstaff et al., Phys. Lett. **B412**, 225–234 (1997).
25. PLUTO Collab., C. Berger et al., Phys. Lett. **142B**, 111–118 (1984); Nucl. Phys. **B281**, 365–380 (1987).
26. TASSO Collab., M. Althoff et al., Z. Phys. **C31**, 527–535 (1986).
27. TPC/2γ Collab., H. Aihara et al., Z. Phys. **C34**, 1–13 (1987).
28. TOPAZ Collab., K. Muramatsu et al., Phys. Lett. **B332**, 477–487 (1994).
29. DELPHI Collab., I. Tyapkin, in *Photon '97, Egmond aan Zee*, eds. A. Buijs and F.C. Erné, pages 26–30, World Scientific, 1998.
30. L3 Collab., F.C. Erné, these proceedings.
31. E. Witten, Nucl. Phys. **B120**, 189–202 (1977).
32. PLUTO Collab., C. Berger et al., Phys. Lett. **142B**, 119–124 (1984).
33. M. Glück, E. Reya, and M. Stratmann, Phys. Rev. **D51**, 3220–3229 (1995).
34. J. Bartels, A. De Roeck, and H. Lotter, Phys. Lett. **B389**, 742–748 (1996); J. Bartels, A. De Roeck, C. Ewerz, and H. Lotter, hep-ph/9710500; S.J. Brodsky, F. Hautmann, and D.E. Soper, Phys. Rev. **D56**, 6957–6979 (1997); Phys. Rev. Lett. **78**, 803–806, Erratum–ibid **79** 3544 (1997).
35. V.S. Fadin and L.N. Lipatov, Phys. Lett. **B429**, 127–134 (1998); G. Camici and M. Ciafaloni, Phys. Lett. **B430**, 349–354 (1998).
36. S.J. Brodsky et al., hep-ph/9901229.

37. M. Boonekamp, A. De Roeck, C. Royon, and S. Wallon, hep-ph/9812523.
38. L3 Collab, M. Acciarri et al., Phys. Lett. **B453**, 333–342 (1999).
39. L3 Collab., P. Achard, these proceedings.
40. OPAL Collab., M. Przybycień, these proceedings.